BIOCHEMISTRY
including biophysical chemistry & molecular biology

Article

pubs.acs.org/biochemistry

TNFR-Associated Factor-2 (TRAF2): Not Only a Trimer

Arianna Ceccarelli,[†] Almerinda Di Venere,[†,§] Eleonora Nicolai,[†,§] Anastasia De Luca,[†,§] Velia Minicozzi,[‡] Nicola Rosato,[†,§] Anna Maria Caccuri,[*,†,§] and Giampiero Mei[*,†,§]

[†]Department of Experimental Medicine and Surgery, University of Rome Tor Vergata, Via Montpellier 1, 00133 Rome, Italy

[‡]Physics Department, INFN University of Rome Tor Vergata, Via della Ricerca Scientifica 1, 00133 Rome, Italy

[§]The NAST Centre for Nanoscience & Nanotechnology & Innovative Instrumentation, University of Rome Tor Vergata, Via della Ricerca Scientifica 1, 00133 Rome, Italy

S *Supporting Information*

ABSTRACT: TNF receptor-associated factors (TRAFs) are characterized by an oligomeric structure that plays a fundamental role in the binding process with membrane receptors. In this work, we studied the trimer-to-monomer (T ↔ 3M) equilibrium transition of the TRAF2 C-terminal domain using both chemical (dilution/guanidinium hydrochloride) and mechanical stress (high pressure) to induce the dissociation of the native protein into subunits. The experimental results and computer simulations indicate that stable monomers exist and that their population accounts for 15% of the total TRAF2 molecules already at a physiological intracellular concentration (≈1 μM), being instead the predominant species in the nanomolar concentration range. Because the total amount of TRAF2 changes during a cell cycle, the monomer−trimer equilibrium can be crucial for regulating the activities of TRAF2 *in vivo*.

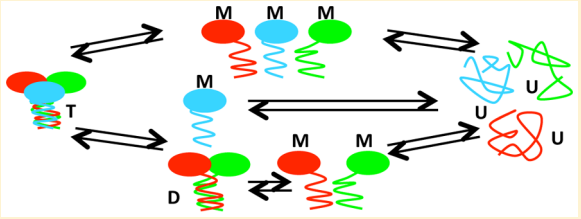

Receptor proteins play a key role in the recognition of chemical signals. In most cases, these systems are formed by complex aggregates of several proteins often constituted by multiple, identical subunits. Binding of trimeric cytokines to tumor necrosis factor receptors (TNFRs) triggers the receptor trimerization and the assembly of multicomponent receptor-associated signaling complexes. The TNF ligands and cognate receptors are involved in diverse biological processes ranging from the induction of cell death to stimulation of immunity and inflammation.[1,2] Key players in TNFR signaling are TNF receptor-associated factor proteins (TRAFs) that can be recruited to activated TNF receptors either by direct interactions with the receptors or indirectly via the adaptor protein TRADD.[3−5] The characterization of the association mechanism of these proteins is therefore crucial for understanding the signaling process in which they are involved. Most TRAF proteins share a common domain organization; the amino-terminal domain contains RING finger and several zinc finger motifs, while the carboxy-terminal portion is subdivided into a TRAF-N domain, characterized by a coiled-coil structure, and a highly conserved TRAF-C domain.[6] Several methods have been utilized to detail the oligomerization states of TRAF proteins and explain the signal transduction following the recruitment of TRAF to receptors. Gel-filtration, sodium dodecyl sulfate−polyacrylamide gel electrophoresis (SDS−PAGE), equilibrium sedimentation, and dynamic light scattering suggested that the carboxy-terminal TRAF domain (construct containing residues 310−501) forms a homotrimer in solution. Moreover, X-ray structure analysis revealed that the TRAF domain has the shape of a mushroom with the TRAF-C domain as the cap and the coiled-coil TRAF-N domain as the stalk.[6] The TRAF-C domain alone is not sufficient for TRAF self-oligomerization, and the TRAF-N domain contributes to stabilizing the oligomer by increasing the buried surface area; in fact, shortening the TRAF-N domain (construct containing residues 342−501) produces monomeric species.

The oligomeric structure of TRAFs plays a major role in binding with the upstream receptors. In fact, TRAF molecules show low affinities for the monomeric receptor peptides[7] and likely do not associate with inactive receptors. Conversely, ligand binding and receptor trimerization allow the simultaneous interaction with TRAFs, thus explaining the response of TRAF molecules to the activation of several TNF receptors. In addition, the carboxy-terminal TRAF domain structure affects clustering of the amino-terminal regions. In fact, in the absence of the carboxy-terminal TRAF domain, the amino-terminal portions (residues 1−133) form only dimers both in crystal lattices and in solution.[8] The amino-terminal region is required for downstream signaling, and its clustering is sufficient for activating all of the downstream protein kinases that transduce TNF-α and IL-1 signals resulting in the induction of their target genes.[9] The recruitment of TRAF2 to TNF receptors results in the activation of different mitogen-activated protein kinase kinase kinases (MAP3Ks) that lie at the apex of MAPK cascades.

Received: June 17, 2015
Revised: September 18, 2015
Published: September 21, 2015

DOI: 10.1021/acs.biochem.5b00674
Biochemistry 2015, 54, 6153−6161

Among the MAP3Ks activated by TRAF2 are mixed-lineage protein kinase 3 (MLK3) and apoptosis signal-regulating kinase 1 (ASK1), which directly associate with TRAF and are responsible for the immediate and persistent activation of JNK, respectively.[10] One of the most important MAP3Ks activated by TRAF2 is MEKK1; binding of MEKK1 to the TRAF2 amino-terminal effector domain results in its clustering and autophosphorylation and in the activation of the downstream JNK/p38, NF-kB, and ERK pathways.[9] Characterizing at the molecular level the protein−protein interactions involving TRAF2 is particularly important, because deregulation of these MAPK signaling has been implicated in the pathogenesis of many human diseases, including neurodegenerative disorders and cancer.[11,12]

It has been suggested that the MAPK signaling by TNFRs follows a two-stage mechanism: first assembly of a multiprotein complex at the receptor intracellular domain and then translocation of the complex to the cytosol where MAP3K substrates are located.[5] In this contest, TRAF proteins may serve as a docking platform for several components situated in the signaling pathway, ensuring precise regulation of signaling by colocalization of successive molecules of the cascade. A natural inhibitor of the signaling mediated by TRAF2 is glutathione transferase GSTP1-1 that sequesters TRAF2 in a protein−protein complex and inhibits its interaction with MAP3Ks.[13,14] If the homotrimeric organization appears to be a prerequisite for the interaction of TRAF2 with receptors, we cannot exclude the possibility of a different molecular organization in the cytoplasm. In this work, we performed a detailed investigation of the oligomeric state of TRAF2 under different experimental conditions, demonstrating that an equilibrium between multimeric and monomeric species exists place in solution. The amount of monomeric or oligomeric TRAF2 depends on its intracellular concentration and may vary during different phases of the cell cycle. Our evidence lays the basis for further studies aimed at understanding the pleiotropic effects mediated by TRAF2 in this complex scenario.

EXPERIMENTAL PROCEDURES

Expression and Purification of TRAF2. *Escherichia coli* BL21(DE3) cells were transformed with the His-tagged human TRAF2 C-terminal domain (residues 310−501) construct and grown in Luria broth medium containing 30 μg/mL kanamycin sulfate.[14] When the absorbance at 600 nm reached 0.5, the expression of TRAF2 was induced by the addition of 1 mM isopropyl 1-thio-β-galactopyranoside. Cells were grown for 18 h at 25 °C, harvested by centrifugation, and resuspended in lysis buffer [20 mM Tris-HCl (pH 8.0), 150 mM NaCl, 20 mM imidazole, 10% glycerol, 1 mM DTT, and EDTA-free inhibitor of protease]. After the cells had been sonicated and centrifuged, the cellular extract was loaded on a 10 mL Ni-NTA column pre-equilibrated with lysis buffer and the protein was eluted using a linear gradient consisting of 50 mL of lysis buffer and 50 mL of the same buffer containing 500 mM imidazole. Imidazole was then removed from the TRAF2 sample by filtration through a Sephadex G25 column (GE Healthcare Life Science, Chalfont St. Giles, U.K.) pre-equilibrated with 20 mM Tris-HCl (pH 7.6) containing 150 mM NaCl and 10% glycerol. The TRAF2 content and its purity were analyzed in the eluted fractions by SDS−PAGE. The protein concentration was determined by measuring the absorbance at 280 nm and using an extinction coefficient of 17780 M^{-1} cm^{-1} for TRAF2 monomers. Proteins were stored at −80 °C.

Steady-State and Dynamic Fluorescence. Steady-state emission spectra were recorded on a K2-ISS (ISS, Inc., Champaign, IL) photon counting fluorometer. In high-pressure measurements, the same instrument was used, equipped with the ISS high-pressure cell. The dissociation curves were obtained by measuring the ratio between the intrinsic fluorescence signals at two different emission wavelengths (F_{350}/F_{308}) and the normalized data fitted according to a two-state T ↔ 3M equilibrium model, using the solution of the following equation (see the Supporting Information):

$$\frac{3}{K_d}[M_0]^3 f_M^{\ 3} + f_M - 1 = 0 \quad (1)$$

where $[M_0]$ is the total subunit concentration, f_M the fraction of monomers at pressure P, and K_d the equilibrium constant [$K_d = e^{(-\Delta G_0 + \Delta V p)/(RT)}$, ΔG_0 and ΔV being the free energy and volume changes, respectively].[15]

A three-state T ↔ D + M ↔ 3M equilibrium model has been also considered, yielding (see the Supporting Information):

$$\frac{3}{K_1 K_2}[M_0]^3 f_M^{\ 3} + \frac{2[M_0]}{K_2} f_M^{\ 2} + f_M - 1 = 0 \quad (2)$$

where K_1 and K_2 are the equilibrium constants of the two steps.

The fits were performed by inserting the solutions of eqs 1 and 2 into the user-defined fitting function routine of Origin Pro8 (OriginLab, Northampton, MA).

An independent evaluation of the volume change, ΔV_C, was also obtained, taking advantage of the concentration-dependent displacement of the dissociation curves:[16]

$$\Delta P_{1/2} = (n - 1)\frac{RT}{\Delta V_C} \ln \frac{C_2}{C_1}$$

Dynamic fluorescence parameters (lifetimes and rotational correlation times) were obtained using the phase-shift and demodulation technique on a KOALA-ISS fluorometer equipped with GLAN Thompson polarizers. The excitation source was a 300 nm laser diode, while emission was collected through a 330 WG cutoff filter to avoid scattering. Measurements have been performed using a total subunit concentrations of ∼20 and ∼5 μM. Any attempt to use more diluted samples in the anisotropy measurements failed because the small number of counts yielded a very poor signal-to-noise ratio. The amplitude, θ, of the segmental tryptophan movement was estimated from the relationship

$$\theta = \arccos\left[\left(\sqrt{1 + 8\sqrt{F_1}} - 1\right)/2\right]$$

where a conic trajectory was assumed and the limiting anisotropy value approximated to fraction F_1 of the longer anisotropy decay component.[17]

Fluorescence Correlation Spectroscopy (FCS). FCS measurements were performed on a Nikon inverted microscope using the ISS-ALBA fluorescence correlation spectrometer. The excitation source (set at 880 nm) was a two-photon Ti:sapphire mode-locked laser (Chameleon Ultra, Coherent Inc., Santa Clara, CA), and alignment was achieved using an 8 nM solution of rhodamine 110. The data points of the autocorrelation function (resulting from the average of three or four independent experiments) were fitted using a Gaussian−Lorentzian intensity profile distribution.[18]

Equilibrium Unfolding Measurements. Equilibrium unfolding measurements were performed after an overnight

DOI: 10.1021/acs.biochem.5b00674
Biochemistry 2015, 54, 6153−6161

incubation, at 4 °C, of TRAF2 samples in the presence of different amounts of ultrapure guanidinium hydrochloride (Sigma, St. Louis, MO). Steady-state fluorescence and circular dichroism (CD) spectra (recorded on a JASCO J-700 spectropolarimeter) were used to characterize the unfolding transition at different TRAF2 concentrations. The experimental data have been fitted taking into account the presence of partially folded monomeric intermediates according to the denaturation scheme

$$T \leftrightarrow 3M \leftrightarrow 3U$$

using the solution of the following equation:

$$\frac{3}{K_1 K_2^{\,3}}[M_0]^2 f_U^{\,3} + \left(1 + \frac{1}{K_2}\right) f_U - 1 = 0 \quad (3)$$

where f_U is the fraction of fully unfolded monomers. The fit was performed using Origin Pro8.

Molecular Dynamics (MD). TRAF2 monomer has been studied by means of classical MD simulations. The starting configuration is one of the monomers of the X-ray diffraction structure[19] [Protein Data Bank (PDB) entry 1CA4].

MD simulations are performed employing the GROMACS package[20−23] and GROMOS43A1 force field[24] and are conducted in the *NpT* ensemble. The temperature is held fixed at 300 K using the v-rescale thermostat[25] with a coupling time of 0.1 ps. The pressure is kept constant at the reference pressure of 1 bar with a coupling time of 1 ps and an isothermal compressibility of 4.5×10^{-5} bar^{-1}, exploiting the features of the Berendsen barostat.[26] The single-point charge (SPC) model is used for water molecules. The simulation box is cubic (with a side of 11.9 nm); TRAF2 monomer is immersed in 55245 water molecules, and an appropriate number of Na^+ or Cl^- counterions are added to have a wholly neutral system. MD simulations are performed at neutral pH.[a] Periodic boundary conditions are used throughout the simulation, and the particle mesh Ewald algorithm is employed to deal with the long-range Coulomb interactions.[27] A time step of 2 fs was used. A nonbond pair list cutoff of 1.4 nm was used, and the pair list was updated every 10 steps. TRAF2 monomer is initially relaxed in vacuum via a steepest descent minimization. Then the appropriate amount of counterions and water is added. At this point, the solvent is relaxed by a few steps (10 ps) of *NVT* MD at 200 K, leaving the solute untouched. Then the whole system, solute and solvent, is equilibrated for 50 ps in the *NVT* ensemble at 300 K. This is the situation from which the final 120 ns long *NpT* MD simulation at 300 K is started.

Analysis of the Intracellular Concentration of TRAF2. A fixed number of U-2OS cells (approximately 7.5×10^4) was lysed as previously reported[28] and subjected to 12% SDS−PAGE together with known amounts of the TRAF2 recombinant protein. Proteins were then transferred to PVDF membranes (Millipore, Billerica, MA). A polyclonal anti-TRAF2 antibody raised against the C-terminal domain (Cell Signaling) was used as the primary antibody. Anti-rabbit secondary antibody (Cell Signaling) was revealed with ECL LiteAblot Extend (EuroClone, Milan, Italy). ImageJ software was used to analyze the band intensities and calculate the protein concentration of the unknown sample by comparison to the intensities of the known samples.

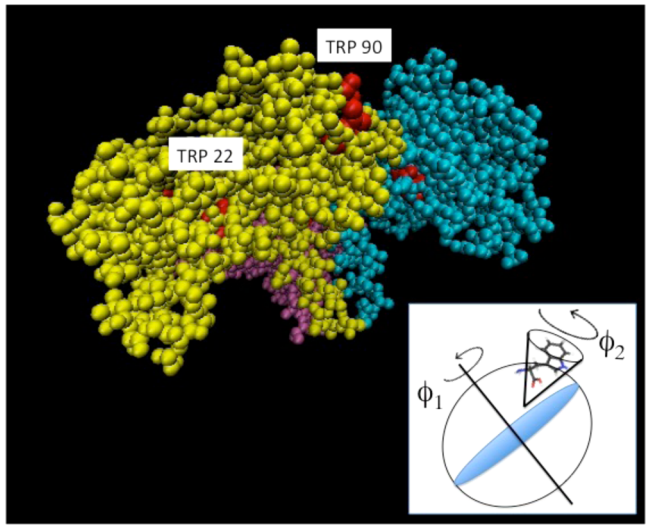

Figure 1. 3D cartoon representation (PDB entry 1ca4) of the TRAF2 trimer. The tryptophan residues contained in each subunit are colored red. The two-rotational correlation time model used to fit the anisotropy decay is sketched in the inset, showing the overall (ϕ_1) and local (ϕ_2) movements.

RESULTS AND DISCUSSION

Characterization of TRAF2 Dynamics in the Micromolar Concentration Range. The aggregation state of TRAF2 in solution has been studied by dynamic fluorescence spectroscopy, measuring the protein rotational correlation time.[17] This task was achieved using the intrinsic fluorescence of the two tryptophan residues contained in each TRAF2 subunit and located in the C-terminal domain, a large "cap" that characterizes the protein three-dimensional (3D) structure (Figure 1). The fluorescence decay was characterized by two fluorescence lifetime distributions, namely, a minor (22%) component centered around $\tau_1 = 1.0 \pm 0.2$ ns and a major contribution (78%) at $\tau_2 = 6.0 \pm 0.5$ ns, yielding an average lifetime value of ∼5.2 ns. In a separate experiment, plane-polarized light was used to excite the TRAF2 fluorophores and the degree of depolarization in the emission fluorescence measured, to detect movements taking place in the range of the excited-state lifetimes. Using a total subunit concentration of ∼20 μM, an exponential anisotropy decay was obtained (data not shown), which was characterized by two distinct components. The first one, $\phi_1 = 29 \pm 2$ ns (fractional contribution $F_1 = 0.75$), corresponding to a slow movement, can be ascribed to the tumbling of the whole protein (Figure 1, inset), being very close to the rotational correlation time expected for a hydrated spherical molecule ($\phi_{sph} = 25$ ns) with the same molecular weight[29] (60000 Da).

The second component [$\phi_2 = 0.6 \pm 0.1$ ns ($F_2 = 0.25$)] is instead diagnostic of a much faster movement and is compatible with the local flexibility of amino acid side chains.[17] Assuming a conic trajectory, the estimated wobbling cone amplitude describing such tryptophan fast dynamics (Figure 1, inset) results in (see Experimental Procedures) $\theta = 24°$, a value that suggests spatially restricted movements. This finding is in line with the location of the TRAF2 tryptophan residues, both almost buried within the protein matrix (Figure 1), their exposed surface being only 8% (Trp22) and 10% (Trp90). When a more diluted sample was taken into account (total subunit concentration of ≈5 μM), a third rotational correlation

DOI: 10.1021/acs.biochem.5b00674
Biochemistry 2015, 54, 6153−6161

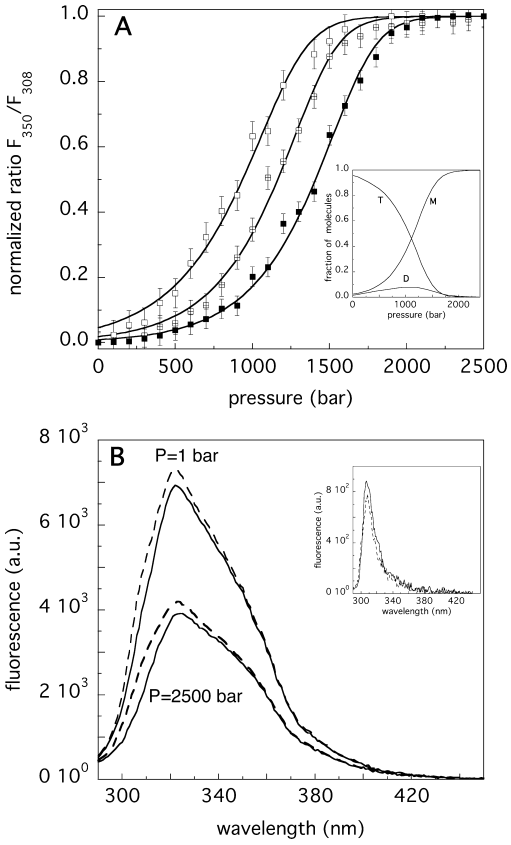

Figure 2. (A) Pressure-induced dissociation curves of TRAF2 at different concentrations (namely, 0.23, 2.3, and 7 μM, from left to right, respectively). The solid lines represent the best fit obtained assuming a simple T ↔ 3M equilibrium process. The inset shows the fractional contribution of monomers M, dimers D, and trimers T, obtained fitting the data of 2.3 μM TRAF2 with the T ↔ D + M ↔ 3M model. (B) Steady-state fluorescence spectra at different excitation wavelengths (292 nm, solid line; 275 nm, dashed line) under atmospheric- and high-pressure conditions ([T] = 7 μM). In the inset, the difference spectra at 1 and 2500 bar are reported.

Table 1. Best Fit Parameters of the TRAF2 Dissociation Curves Reported in Figure 2

$[M_0]^a$ (μM)	ΔV_{fit} (mL/mol)	ΔG_{diss} (kcal/mol)	$[M]/[M_0]$
0.65	215 ± 11	20.4 ± 0.5	0.18
2.3	224 ± 7	20.5 ± 0.4	0.10
7.0	220 ± 6	20.6 ± 0.3	0.06

[a]Total subunit concentration.

component (ϕ_3 = 8.6 ± 0.5 ns) was necessary to fit the data, compatible with the presence of monomeric species with a molecular weight of 20000 Da. The percentage of monomers estimated from the fractional contribution of ϕ_3 to the total anisotropy decay was $[M]_{\%}$ = (7.8 ± 0.7)%.

In conclusion, anisotropy measurements provide evidence that TRAF2 is essentially a trimer above 20 μM, while the presence of monomers becomes detectable already around 5 μM.

Pressure-Induced Dissociation of TRAF2 Trimers. Oligomeric proteins can be separated into monomeric subunits using a high hydrostatic pressure.[30] This approach has several advantages with respect to temperature-, pH-, or chaotropic agent-induced dissociation, depending solely on the change in volume occurring in the process.[30] As a consequence, only a partial perturbation of the system (protein and buffer) is produced, and the complete unfolding of monomers is often avoided[31] in a manner independent on their size.[32,33] The dissociation of native TRAF2 has been investigated at 25 °C through steady-state intrinsic fluorescence. In particular, we used a ratiometric approach, measuring the protein intrinsic fluorescence at 350 and 308 nm in the range of 1−2500 bar. As shown in Figure 2A, sigmoidally shaped transitions have been obtained at three different protein concentrations, demonstrating that an equilibrium between multimeric and monomeric species exists. Thus, assuming a two-state transition process, the data have been fitted according to a simple, T ↔ 3M, monomerization model. The analysis reveals that the free energy of dissociation is on the order of 20 kcal/mol (Table 1), a value comparable to that obtained for most oligomers studied in the past several years.[34−36] The corresponding dissociation constant at atmospheric pressure ($K_0 \approx 7.6 \times 10^{-16}$ M^2) allows calculation of the ratio between the concentration of monomers and trimers. These values, reported in Table 1, demonstrate that the presence of monomeric species is no more negligible at 1 bar when the protein concentration is lower than a few micromolar.

The volume change associated with the dissociation process ($\Delta V_{fit} \approx$ 220 mL/mol) obtained from the data fit (Table 1) suggests that a large hydration at the subunit interface occurs, as the monomers are taken apart. Another estimation of this parameter, ΔV_C, can be obtained by evaluating the displacement of the dissociation curves ($\Delta P_{1/2}$) due to a change in the protein concentration (see Experimental Procedures). In this last case, the data in Figure 2A yield a ΔV_C of 228 ± 17 mL/mol. The two independent approaches demonstrate that $\Delta V_{fit} \approx \Delta V_C$, indicating that no conformational heterogeneity occurs

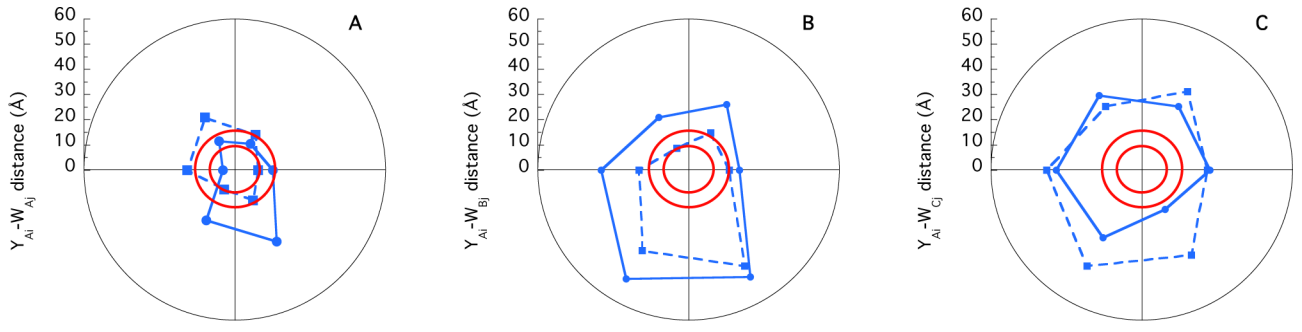

Figure 3. Plot of the crystallographic distances between each of the six tyrosines present in subunits A−C and each tryptophan residue of subunit A. Trp22 and Trp90 are assumed to be in the center of each plot. The six Tyr residues and Trp90 and Tyr residues and Trp22 are connected with solid and dashed lies, respectively. The red circles represent the typical Tyr−Trp Förster distance.

DOI: 10.1021/acs.biochem.5b00674
Biochemistry 2015, 54, 6153−6161

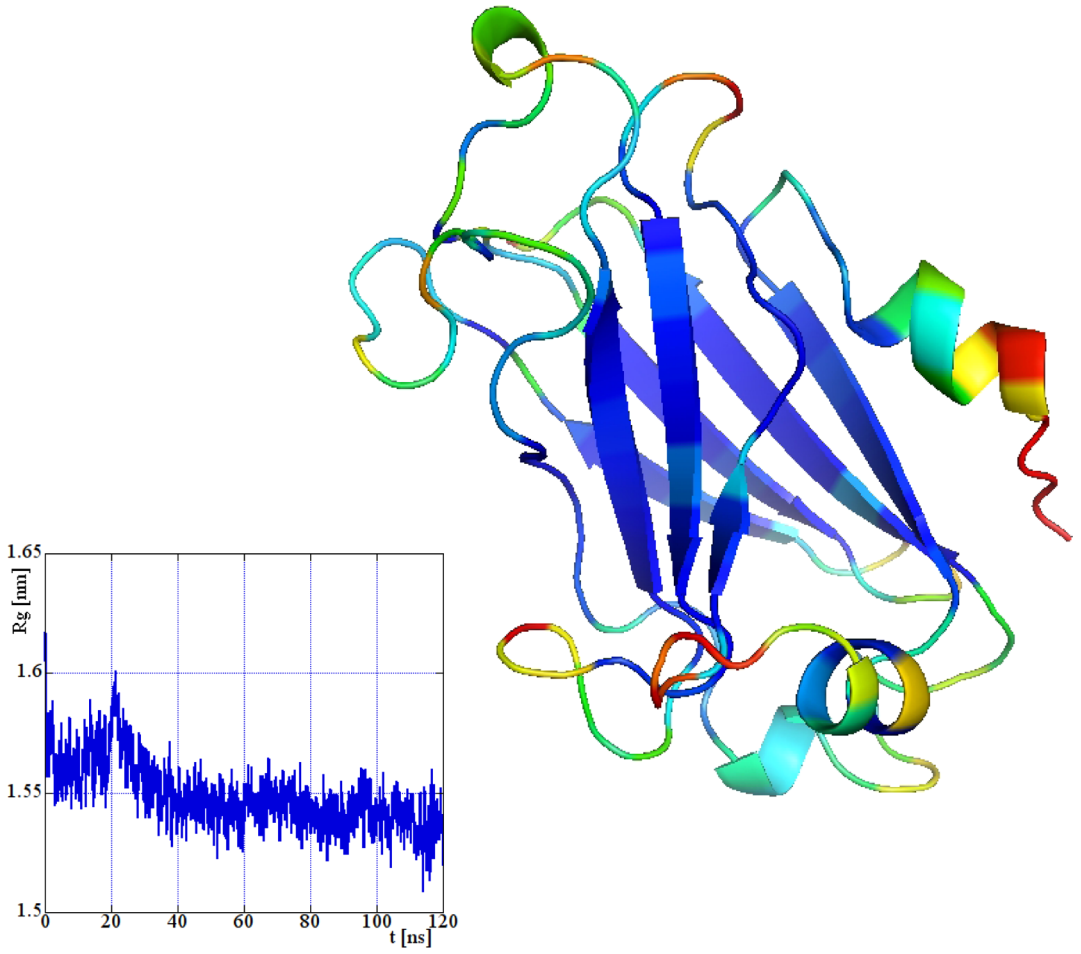

Figure 4. Average structure of TRAF2 monomer at 300 K. Colors are distributed over the range of *b* factor values, with blue representing the lowest (most stable) and red the highest (most fluctuating) protein segment. The inset shows the TRAF2 gyration radius at 300 K as a function of simulation time.

and that dissociation takes place according to the law of mass action,[16] in the micromolar concentration range.

The possibility that a dimeric species, D_2, is also present has been tested fitting the data with a more complicated model, namely, T ↔ D + M ↔ 3M. The quality of the fit did not improve, as similar χ^2 values were obtained (data not shown), despite this model requiring two additional free variables with respect to the simpler T ↔ 3M scheme (see Experimental Procedures). For each of the three dissociation curves, the fractions of trimers, dimers, and monomers have been obtained and the results attained at the intermediate TRAF2 initial concentration (2.3 μM) reported in the inset of Figure 2A. These findings indicate that the presence of a dimeric species is negligible and that the detachment of the first subunit from the native trimeric protein is immediately followed by a further dissociation of the remaining dimer into monomeric species.

Structural information about the TRAF2 monomers can be guessed comparing the fluorescence spectra recorded at 1 and 2500 bar. When the excitation wavelength was set at 292 nm (to avoid the contribution of tyrosines), both spectra showed a maximum around 320 nm (Figure 2B), which is a typical feature of tryptophan-buried residues, diagnostic of a folded 3D structure. On the other hand, excitation at 275 nm yielded a similar result, the only difference being an extra shoulder in the spectral range of 300−325 nm. The difference spectra (excitation at 275 nm, excitation at 292 nm) demonstrate that this blue-shifted emission is characterized by a low intensity (a few hundred counts) and an emission peak centered around 307 nm (Figure 2B, inset). Such findings demonstrate that the contribution of the six tyrosines is very weak, probably because of an efficient energy transfer to tryptophan residues. This hypothesis is in line with the tyrosine−tryptophan distances evaluated on the basis of the available crystallographic structure. Assuming tyrosines as donors and tryptophans as acceptors, the optimal R_0 Förster distance (i.e., at which 50% of the maximal transfer efficiency occurs) is estimated to be ≈9 Å.[29] As shown in Figure 3A, at least eight of the 12 possible Tyr−Trp couples within the same subunit are 9−18 Å apart, i.e., between R_0 and $2R_0$, confirming that an efficient intrasubunit energy transfer process might occur. On the other hand, the interaction among fluorophores belonging to different subunits seems to be more difficult because of the larger distances that exist between donors and acceptors (Figure 3B,C). The overlap of the difference fluorescence spectra measured at 1 and 2500 bar (Figure 2B, inset) therefore demonstrates that protein dissociation does not affect the tyrosine-to-tryptophan energy transfer process. Such findings indicate that the isolated monomers produced at 2500 bar retain the tertiary structure of the tryptophans environment that they display in the native, oligomeric molecule.

Exploring the Stability of TRAF2 Monomer *in Silico*. The possibility that TRAF2 might exist as folded monomer at

DOI: 10.1021/acs.biochem.5b00674
Biochemistry 2015, 54, 6153−6161

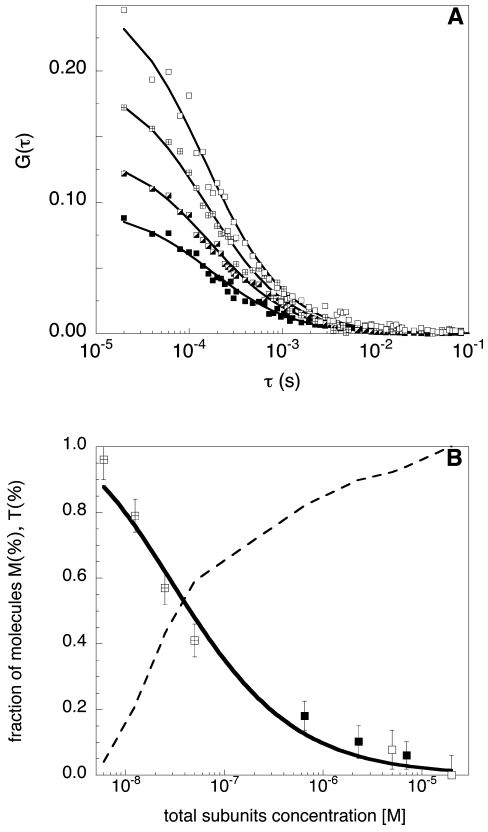

Figure 5. (A) Autocorrelation curves of Alexa488-labeled TRAF2 at different concentrations, namely, 6, 12, 25, and 50 nM (from top to bottom, respectively). The solid lines represent the best fits obtained assuming the presence of two different species, namely, T and M. (B) Fractions of monomers obtained in dynamic anisotropy, high-pressure, and FCS measurements (empty, filled, and crossed squares, respectively) as a function of total subunit concentration. The solid line represents the best theoretical fit yielding a dissociation constant of $(1.4 \pm 0.4) \times 10^{-16}$ M^2. The dotted line represents the trimer percentage.

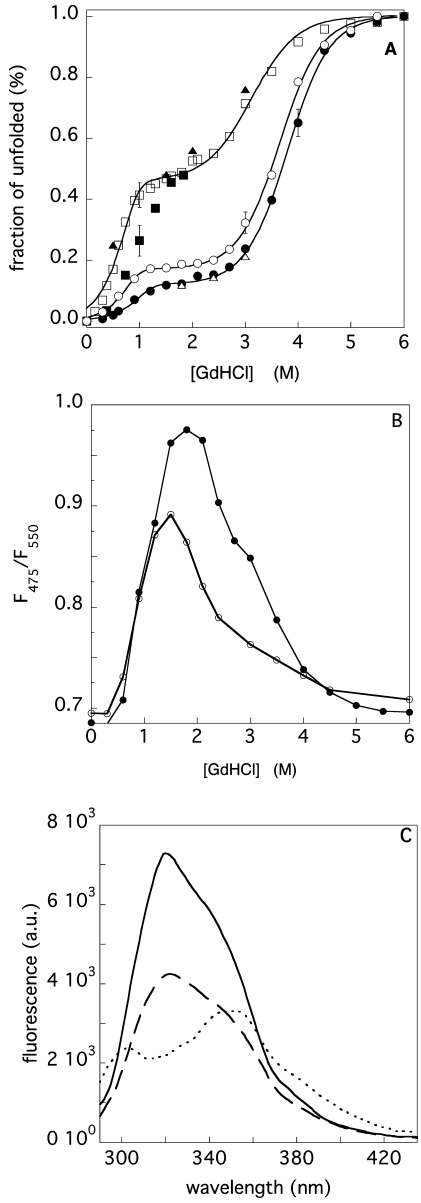

Figure 6. (A) GdHCl-induced unfolding of TRAF2 monitored by CD (squares) and fluorescence (circles). Measurements were repeated at different protein concentrations, namely, 15 (■), 0.8 (□), 3 (●), and 0.3 μM (○). Triangles indicate the reversibility of the process, upon denaturant dilution. (B) ANS fluorescence ratio in the presence of TRAF2 (0.3 μM, solid line; 3.0 μM, gray bars) at increasing GdHCl concentrations. (C) Steady-state fluorescence spectra of TRAF2 at 20 °C and 1 bar in the presence of different levels of GdHCl, namely, 0 (—), 1.5 (– – –), and 6 M (···).

atmospheric pressure has been tested by computer simulation. Briefly, we have performed a 120 ns MD simulation of TRAF2 monomer at 300 K and 1 bar in the *NpT* ensemble starting from one of the monomers of the X-ray diffraction structure[19] (PDB entry 1CA4).

The average structure obtained after a 120 ns simulation is shown in Figure 4. The TRAF2 monomeric subunit becomes folded, with the characteristic β-sandwhich core,[19] and a gyration ratio of ~1.55 nm (Figure 4, inset), diagnostic of a compact and stable 3D globular shape. The resulting diffusion coefficient (D) is 110 μ^2/s.

The most flexible domain is clearly the N-terminal α-domain that also in the trimer crystallographic model is characterized by higher average temperature factors, forming with the α-helices of the other two monomers a coiled-coil mobile domain.[19]

Characterization of TRAF2 Dynamics in the Nanomolar Concentration Range. The equilibrium between monomeric and trimeric TRAF2 has also been studied in the nanomolar concentration range using FCS. Protein samples (from 6 to 50 nM) have been labeled with ALEXA-488 and excited at 880 nm through a two-photon laser beam. The corresponding autocorrelation curves are reported in Figure 5A. The data have been globally fitted using a two-component fitting function, producing diffusion coefficients of ~107 ± 7 and ~69 ± 9 μm^2/s, which correspond to those of monomeric and trimeric TRAF2 molecules, respectively.[37]

The resulting fractional concentrations are reported in Figure 5B together with the values obtained in the micromolar range using high pressure (Table 1) and dynamic anisotropy. The three data sets have been globally fitted according to the T ↔ 3M equilibrium, and the value of the dissociation constant obtained (K_D) was $(1.4 \pm 0.4) \times 10^{-16}$ M^2.

Stability of TRAF2 Trimers. The trimer−monomer equilibrium and the stability of the two species have been further characterized by investigating the effects produced by GdHCl on TRAF2 secondary and tertiary structure using CD

DOI: 10.1021/acs.biochem.5b00674
Biochemistry 2015, 54, 6153−6161

Table 2. Best Fit Parameters of TRAF2 Unfolding Curves Reported in Figure 6

technique	[TRAF2] (μM)	m_1 (kcal M^{-1})	ΔG_1 (kcal/mol)	m_2 (kcal M^{-1})	ΔG_2 (kcal/mol)
CD	0.8	5.5 ± 0.5	18.9 ± 0.6	1.2 ± 0.1	4.3 ± 0.4
fluorescence	0.3	5.9 ± 0.2	20.6 ± 0.6	1.5 ± 0.2	5.6 ± 0.3
fluorescence	3.0	5.3 ± 0.7	18.6 ± 1.4	1.5 ± 0.1	5.7 ± 0.4

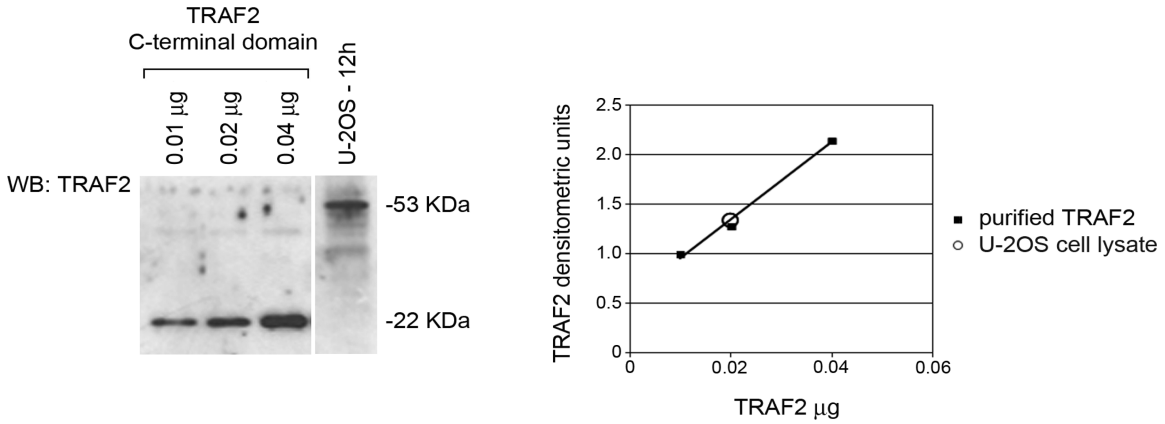

Figure 7. Representative Western blot analysis of TRAF2 expression in U-2OS cells. Protein lysate from a fixed number of U-2OS cells (approximately 7.5 × 10^4) was separated by SDS−PAGE, and expression of TRAF2 was determined by using a polyclonal anti-TRAF2 primary antibody, raised against the C-terminal domain. The amount of intracellular TRAF2 was calculated by using band intensities from known amounts of the TRAF2 recombinant protein (C-terminal domain). The intracellular TRAF2 concentration was calculated by assuming an U-2OS cell volume of 4000 μm^3. Data represent means ± the standard deviation of three independent experiments.

and steady-state fluorescence, respectively. The first part of the unfolding transition (Figure 6A) is dependent on protein concentration, indicating that dissociation is occurring. The data have been therefore fitted according to the T ↔ 3M ↔ 3U scheme, T, M, and U being the native trimer, a monomeric intermediate, and the unfolded molecule, respectively. The parameters obtained (and reported in Table 2) demonstrate that (i) the quaternary interactions account for ≈55% of the total stabilization energy ($\Delta G_{tot} = \Delta G_1 + 3\Delta G_2 \approx 35$ kcal/mol), (ii) monomers have a stable structure characterized by a ΔG_2 value of ∼5 kcal/mol, and (iii) monomerization is a quite cooperative process and is coupled to the partial exposure of the native buried surface to solvent molecules, as demonstrated by the value (≈ 5−6 kcal mol^{-1} M^{-1}) obtained for m_1.[38] This last finding is also confirmed by ANS binding (Figure 6B), which is maximal around 1.5−1.8 M GdHCl, i.e., corresponding to the plateau observed in Figure 6A. The analysis of the steady-state fluorescence spectrum at 1.5 M GdHCl (Figure 6C) demonstrates that it is similar to that obtained at high pressure (Figure 2B) and that it does not show the typical emission peak of tyrosines (305 nm), which instead appears at 6.0 M GdHCl. These results indicate that in the intermediate monomeric species the fluorescence energy transfer process between tyrosines and tryptophans is still very efficient, thus suggesting that the overall 3D structure is similar to that of the native protein. Indeed, a large part of the secondary structure (≈60%) and most of the tertiary interactions (≈85−90%) that characterize the native protein are retained in the monomeric state (Figure 6A). Finally, the similarity of the spectra at 2500 bar and 1.5 M GdHCl provides evidence that both mechanically and chemically induced trimer dissociation lead to the same structural state, as also suggested by the good correspondence between the dissociation energy evaluated from high-pressure measurements [ΔG_{diss} (Table 1)] and the free energy of unfolding that characterizes the first step of the transition [ΔG_1 (Table 2)].

Most of the C-terminal domain of TRAF2 is organized in a β-sandwich core[19] that contains all the tryptophans and tyrosines present in the protein sequence and that resulted in the most stable secondary structure motif from *in silico* simulations (Figure 4). On the other hand, the intensity of the CD spectrum is known to be dominated by α-helices in α/β proteins.[39]

Because TRAF2 dissociation only marginally affects the protein's tertiary interactions (Figures 2B and 6A), it is tempting to speculate that the loosening of the CD signal in the monomeric subunits (Figure 6A) is mainly due to the unfolding of the mobile α-helix present in the N-terminal region, the domain that forms the coiled-coil structure responsible for TRAF2 binding to other molecules.[40]

Intracellular Concentration of TRAF2. The intracellular amount (micrograms) of TRAF2 was determined in human osteosarcoma U-2OS cells, 12 h after plating, by quantitative Western blot analysis. Assuming a TRAF2 molecular weight of 52 kDa (monomer) and an U-2OS cell volume of 4000 μm^3 ∼ 4.0 × 10^{-12} L,[41] we calculated an intracellular TRAF2 concentration of ∼1 μM (Figure 7).

In conclusion, using independent experimental approaches (high-pressure dissociation, dynamic anisotropy, and FCS at atmospheric pressure), we have characterized the monomer−trimer equilibrium of TRAF2 in solution, covering a concentration range that goes from nanomolar to tens of micromolar. At a high protein concentration (20 μM), dynamic anisotropy measurements provide evidence that the protein is essentially a trimer, while dissociation into subunits occurs already at 5 μM. The amount of monomeric or oligomeric TRAF2 depends on its intracellular concentration *in vivo*. Quantitative Western blot analysis performed on proliferating U-2OS cells indicates that the amount of intracellular TRAF2 is ∼1 μM (monomers). Therefore, on the basis of the calculated dissociation constant [$K_D = (1.4 \pm 0.4) \times 10^{-16}$ M^2], we can predict that the presence of monomers is not negligible at 1

DOI: 10.1021/acs.biochem.5b00674
Biochemistry 2015, 54, 6153−6161

μM, as they account for ∼15% of the total TRAF2 species (Figure 5B). Structural information about the monomeric species has been obtained by high-pressure measurements, indicating that the isolated monomers retain a 3D structure similar to that of the native protein. The possibility that the isolated TRAF2 subunits are stable is also supported by computer simulation analysis and confirmed by unfolding experiments performed at atmospheric pressure.

We have previously shown that the total amount of TRAF2 decreases in G2 and M phases,[14] so that the monomer−trimer equilibrium may also be regulated in a cell cycle-dependent manner. This modulatory mechanism, if confirmed, might play an important role in the multiple TRAF2 activities *in vivo*.

■ ASSOCIATED CONTENT

Supporting Information

The Supporting Information is available free of charge on the ACS Publications website at DOI: 10.1021/acs.biochem.5b00674.

Mathematical derivation of the analytical functions used to fit the data sets (PDF)

■ AUTHOR INFORMATION

Corresponding Authors

*E-mail: caccuri@uniroma2.it. Phone: (+39) 0672596204. Fax: (+39) 0672596468.

*E-mail: mei@med.uniroma2.it. Phone: (+39) 0672596464. Fax: (+39) 0672596468.

Author Contributions

A.M.C. and G.M. contributed equally to this work.

Funding

This work was supported by Associazione Italiana per la Ricerca sul Cancro (AIRC), Project IG-10598 (A.M.C.).

Notes

The authors declare no competing financial interest.

■ ACKNOWLEDGMENTS

We thank Dr. Alessandra Filabozzi for helpful discussion and suggestion in running software analysis.

■ DEDICATION

This paper is dedicated to the memory of Professor Donatella Barra.

■ ABBREVIATIONS

TRAFs, TNF receptor-associated factors; TNFRs, tumor necrosis factor receptors; MAP3K, mitogen-activated protein kinase kinase kinase; MLK3, mixed-lineage protein kinase 3; ASK1, apoptosis signal-regulating kinase 1; JNK, c-Jun N-terminal kinase; GSTP1-1, glutathione transferase P1-1; FCS, fluorescence correlation spectroscopy; GdHCl, guanidinium hydrochloride; CD, circular dichroism; MD, molecular dynamics; SPC, single-point charge.

■ ADDITIONAL NOTE

[a]This means that the protonation state of the monomer was chosen so that the N-terminus, arginine, and lysine are protonated and positively charged while the C-terminus, glutamic acid, and aspartic acid are deprotonated and negatively charged. This choice corresponds to the expected protonation state of free amino acids at neutral pH.

■ REFERENCES

(1) Bremer, E. (2013) Targeting of the tumor necrosis factor receptor superfamily for cancer immunotherapy. *ISRN Oncol. 2013*, 371854.

(2) Chen, G., and Goeddel, D. V. (2002) TNF-R1 signaling: a beautiful pathway. *Science 296* (5573), 1634−1635.

(3) Park, Y. C., Ye, H., Hsia, C., Segal, D., Rich, R. L., Liou, H.-C., Myszka, D. G., and Wu, H. (2000) A Novel Mechanism of TRAF Signaling Revealed by Structural and Functional Analyses of the TRADD-TRAF2 Interaction. *Cell 101*, 777−787.

(4) Bradley, J. R., and Pober, J. S. (2001) Tumor necrosis factor receptor-associated factors (TRAFs). *Oncogene 20*, 6482−6491.

(5) Matsuzawa, A., Tseng, P. H., Vallabhapurapu, S., Luo, J. L., Zhang, W., Wang, H., Vignali, D. A., Gallagher, E., and Karin, M. (2008) Essential cytoplasmic translocation of a cytokine receptor-assembled signaling complex. *Science 321* (5889), 663−668.

(6) Wu, H., Park, Y. C., YE, H., and Tong, L. (1999) Structural Studies of Human TRAF2. *Cold Spring Harbor Symp. Quant. Biol. 64*, 541−550.

(7) Ye, H., Park, Y. C., Kreishman, M., Kieff, E., and Wu, H. (1999) The Structural Basis for the Recognition of Diverse Receptor Sequences by TRAF2. *Mol. Cell 4* (3), 321−330.

(8) Yin, Q., Lamothe, B., Darnay, B. G., and Wu, H. (2009) Structural basis for lack of E2 interaction in the RING of TRAF2. *Biochemistry 48* (44), 10558−10567.

(9) Baud, V., Liu, Z. G., Bennett, B., Suzuki, N., Xia, Y., and Karin, M. (1999) Signaling by proinflammatory cytokines: oligomerization of TRAF2 and TRAF6 is sufficient for JNK and IKK activation and target gene induction via an amino-terminal effector domain. *Genes Dev. 13* (10), 1297−1308.

(10) Sondarva, G., Kundu, C. N., Mehrotra, S., Mishra, R., Rangasamy, V., Sathyanarayana, P., Ray, R. S., Rana, B., and Rana, A. (2010) TRAF2-MLK3 interaction is essential for TNF-alpha-induced MLK3 activation. *Cell Res. 20* (1), 89−98.

(11) Song, J., Park, K. A., Lee, W. T., and Lee, J. E. (2014) Apoptosis signal regulating kinase 1 (ASK1): potential as a therapeutic target for Alzheimer's disease. *Int. J. Mol. Sci. 15* (2), 2119−2129.

(12) Kitanaka, C., Sato, A., and Okada, M. (2013) JNK Signaling in the Control of the Tumor-Initiating Capacity Associated with Cancer Stem Cells. *Genes Cancer 4* (9−10), 388−396.

(13) Wu, Y., Fan, Y., Xue, B., Luo, L., Shen, J., Zhang, S., Jiang, Y., and Yin, Z. (2006) Human glutathione S-transferase P1−1 interacts with TRAF2 and regulates TRAF2-ASK1 signals. *Oncogene 25* (42), 5787−5800.

(14) De Luca, A., Mei, G., Rosato, N., Nicolai, E., Federici, L., Palumbo, C., Pastore, A., Serra, M., and Caccuri, A. M. (2014) The fine-tuning of TRAF2−GSTP1−1 interaction: effect of ligand binding and *in situ* detection of the complex. *Cell Death Dis. 5*, e1015.

(15) Weber, G., and Drickamer, H. G. (1983) The effect of high pressure upon proteins and other biomolecules. *Q. Rev. Biophys. 16* (1), 89−112.

(16) Foguel, D., Silva, J. L., and de Prat-Gay, G. (1998) Characterization of a partially folded monomer of the DNA-binding domain of human papillomavirus E2 protein obtained at high pressure. *J. Biol. Chem. 273* (15), 9050−9057.

(17) Lakowicz, J. R. (1999) in *Principles of Fluorescence Spectroscopy*, 2nd ed., pp 321−345, Kluwer Academic/Plenum Publischers, New York.

(18) Berland, K. M., So, P. T., and Gratton, E. (1995) Two-photon fluorescence correlation spectroscopy: method and application to the intracellular environment. *Biophys. J. 68* (2), 694−701.

(19) Park, Y. C., Burkitt, V., Villa, A. R., Tong, L., and Wu, H. (1999) Structural basis for self-association and receptor recognition of human TRAF2. *Nature 398*, 533.

(20) Berendsen, H. J. C., van der Spoel, D., and van Drunen, R. (1995) GROMACS: A message-passing parallel molecular dynamics implementation. *Comput. Phys. Commun. 91*, 43−56.

DOI: 10.1021/acs.biochem.5b00674
Biochemistry 2015, 54, 6153−6161

(21) Lindahl, E., Hess, B., and van der Spoel, D. (2001) GROMACS 3.0: a package for molecular simulation and trajectory analysis. *J. Mol. Model. 7*, 306−317.
(22) van der Spoel, D., Lindahl, E., Hess, B., Groenhof, G., Mark, A. E., and Berendsen, H. J. C. (2005) GROMACS: Fast, flexible, and free. *J. Comput. Chem. 26*, 1701−1718.
(23) Hess, B., Kutzner, C., van der Spoel, D., and Lindahl, E. (2008) GROMACS 4: Algorithms for Highly Efficient, Load-Balanced, and Scalable Molecular Simulation. *J. Chem. Theory Comput. 4*, 435−447.
(24) van Gunsteren, W. F., Billeter, S. R., Eking, A. A., Hiinenberger, P. H., Kriiger, P., Mark, A. E., Scott, W. R. P., and Tironi, I. G. (1996) Biomolecular Simulation. *The GROMOS96 Manual and User Guide*, vdf Hochschulverlag AG an der ETH Zurich, Zurich, and BIOMOS b.v., Groningen, Germany.
(25) Bussi, G., Donadio, D., and Parrinello, M. (2007) Canonical sampling through velocity rescaling. *J. Chem. Phys. 126*, 014101.
(26) Berendsen, H. J. C., Postma, J. P. M., van Gunsteren, W. F., DiNola, A., and Haak, J. R. (1984) Molecular dynamics with coupling to an external bath. *J. Chem. Phys. 81*, 3684−3690.
(27) Darden, T., York, D., and Pedersen, L. (1993) Particle mesh Ewald: An Nlog(N) method for Ewald sums in large systems. *J. Chem. Phys. 98*, 10089−10092.
(28) Sau, A., Filomeni, G., Pezzola, S., Serra, M., D'Aguanno, S., Tregno, F. P., Urbani, A., Serra, M., Pasello, M., Picci, P., Federici, G., and Caccuri, A. M. (2012) Targeting GSTP1−1 induces JNK activation and leeds to apoptosis in cisplatin-sensitive and − resistant human osteosarcoma cell lines. *Mol. BioSyst. 8* (4), 994−1006.
(29) Cantor, C. (1980) in *Biophysical Chemistry, Part II: Techniques for the study of biological structure and function*, pp 451−463, W. H. Freeman and Co., San Francisco.
(30) Silva, J. L., Foguel, D., and Royer, C. A. (2001) Pressure provides new insights into protein folding, dynamics and structure. *Trends Biochem. Sci. 26* (10), 612−618.
(31) Mozhaev, V. V., Heremans, K., Frank, J., Masson, P., and Balny, C. (1996) High pressure effects on protein structure and function. *Proteins: Struct., Funct., Genet. 24*, 81−91.
(32) Perrett, S., and Zhou, J. M. (2002) Expanding the pressure technique: insights into protein folding from combine dure of pressure and chemical denaturants. *Biochim. Biophys. Acta, Protein Struct. Mol. Enzymol. 1595* (1−2), 210−223.
(33) Mei, G., Di Venere, A., Campeggi, F. M., Gilardi, G., Rosato, N., De Matteis, F., and Finazzì-Agrò, A. (1999) The effect of pressure and guanidine hydrochloride on azurine mutated in the hydrophobic core. *Eur. J. Biochem. 265* (2), 619−626.
(34) Mei, G., Di Venere, A., Rosato, N., and Finazi-Agrò, A. (2005) The Importance of being dimeric. *FEBS J. 272* (1), 16−27.
(35) Neet, K. E., and Timm, D. E. (1994) Conformational stability of dimeric proteins: quantitative studies by equilibrium denaturation. *Protein Sci. 3*, 2167−2174.
(36) Rumfeldt, J. A. O., Galvagnion, C., Vassall, K. A., and Meiering, E. M. (2008) Conformational stability and folding mechanisms of dimeric proteins. *Prog. Biophys. Mol. Biol. 98*, 61−84.
(37) Young, M. E., Carroad, P. A., and Bell, R. L. (1980) Estimation of diffusion coefficients of proteins. *Biotechnol. Bioeng. 22*, 947−955.
(38) Myers, J. K., Pace, C. N., and Scholtz, J. M. (1995) Denaturant m values and heat capacity changes: relation to changes in accessible surface areas of protein unfolding. *Protein Sci. 4* (10), 2138−2148.
(39) Fasman, G. D. (1996) *Circular Dichroism and the Conformational Analysis of Biomolecules*, pp 72, Plenum Press, New York.
(40) Zheng, C., Kabaleeswaran, V., Wang, Y., Cheng, G., and Wu, H. (2010) Crystal structures of the TRAF2: cIAP2 and the TRAF1: TRAF2: cIAP2 complexes: affinity, specificity, and regulation. *Mol. Cell 38* (1), 101−113.
(41) Beck, M., Schmidt, A., Malmstroem, J., Claassen, M., Ori, A., Szymborska, A., Herzog, F., Rinner, O., Ellenberg, J., and Aebersold, R. (2011) The quantitative proteome of a human cell line. *Mol. Syst. Biol. 7*, 549.

DOI: 10.1021/acs.biochem.5b00674
Biochemistry 2015, 54, 6153−6161